Research in Pharmaceutical Sciences, June 2019; 14(3):216-227
Received: September 2018
Accepted: May 2019

School of Pharmacy & Pharmaceutical Sciences
Isfahan University of Medical Sciences

Original Article

β-lactoglobulin-irinotecan inclusion complex as a new targeted nanocarrier for colorectal cancer cells

Nooshin Bijari[1,2], Sirous Ghobadi[2], and Katayoun Derakhshandeh[3,*]

[1]*Nano Drug Delivery Research Center, Faculty of Pharmacy, Kermanshah University of Medical Sciences, Kermanshah, I.R. Iran.*
[2]*Department of Biology, Faculty of Science, Razi University, Kermanshah, I.R. Iran.*
[3]*Department of pharmaceutics, School of Pharmacy, Hamadan University of Medical Sciences, Hamadan, I.R. Iran.*

Abstract

Beta-lactoglobulin (β-LG) is a lipocalin family member whose general function appears to be solubilizing and transport of hydrophobic molecules. Some properties such as avalability, ease of purification, and peculiar resistance to acidic environments can make β-LG as a carrier for hydrophobic and acid labile drugs for oral administration. In this protein vehicle, drug could be protected in acidic environment of stomach and then released within the basic small intestine. In this study, the potential of β-LG as a nanocarrier for oral delivery of a potent agent in colorectal cancer treatment, irinotecan, was evaluated. The nanoparticle was prepared by the physical inclusion complex method. Size, drug loading, encapsulation efficiency, and *in vitro* drug release at various pH values were investigated. The optimum formulation showed a narrow size distribution with an average diameter of 139.86 ± 13.75 nm and drug loading about 84.33 ± 5.03%. Based on the results obtained from docking simulation of irinotecan-complex, there are two distinct binding sites in this nanocarrier. Cytotoxicity of this nanocarrier on the HT-29 cancer cell line and AGS was measured by MTT assay. The cytotoxicity experiment showed that the drug-loaded nanocarrier was more effective than free drug. The higher release percent of drug from the β-LG complex at pH 7.4 compared to pH 1.2 indicated that the proposed nanocarrier could be introduced as a suitable nanovehicle for labile drugs in acidic medium targeted for colorectal segment.

Keywords: Beta-lactoglobulin; Colorectal cancer; Irinotecan; Nano drug delivery system.

INTRODUCTION

In recent years, significant progress in drug delivery systems has led to the development of oral delivery of anticancer drugs. Nanoscale oral drug delivery systems has shown potentials to achieve various drug delivery goals by protecting drugs from deterioration in the gastrointestinal tract, facilitating diffusion of drug through intestinal lumen leading to enhancement of drug absorption and modifying drug tissue distribution profile (1). Similar to biopolymers, proteins can be used as the excipients in drug delivery system (2). Beta-lactoglobulin (β-LG) is a protein that is widely used in food industry due to its high nutritional value; also, it is used as foaming, emulsifying, gelling and ligand binding agent. As a globular protein of lipocalin family, β-LG is able to bind small hydrophobic molecules such as fatty acids, retinol and other fat soluble vitamins, isothiocyanates, and various polyphenols while, the other binding sites have not been known until now (3,4). β-LG is a 18 kDa protein consisting of 162 amino acid residues with two disulfide bridges and one unbound cysteine residue (5,6). It consists of nine antiparallel β-strands (β-A to β-I) and one α-helix at the C-terminal end of the molecule. Eight antiparallel β-strands (β-A to β-H) form an antiparallel β-barrel containing conical central cavity as a ligand-binding site.

*Corresponding author: K. Derakhshandeh
Tel: +98-8138381590, Fax: +98-8138381591
Email: k.derakhshandeh@umsha.ac.ir

Access this article online

Website: http://rps.mui.ac.ir

DOI: 10.4103/1735-5362.258488

One surface of the β-barrel consists of strands β-A to β-D and the other surface consists of strands β-E to β-H. The β-barrel is a broad calyx shape with a large fossa lined with hydrophobic residues and has access to bulk solvent. It has a significant affinity to hydrophobic ligands and it functions as a transporter of retinal and fatty acids (7,8). The N-terminal loop closes the calyx form at one end, while the EF loop can close the other end of calyx in low pH condition (9). Therefore, the accessibility to the calyx depends on the pH. The mobile EF loop at the calyx entrance contains residues isoleucine 84 to asparagine 90. When glutamic acid 89 is protonated at low pH, the loop is closed while at higher pH, glutamic acid 89 becomes deprotonated and the loop will be opened (10).

Colorectal cancer is considered resistant to chemotherapy. 5-fluorouracil is an old drug for colon cancer that has been replaced by some new drugs such as raltitrexed, capecitabine, irinotecan, and oxaliplatin. Camptothecin is another anticancer drug isolated from the Chinese Happy Tree (*Camptotheca acuminata*) in the 1960s and its mechanism of action and anticancer potential was identified later. Its mechanism of action is targeting the nuclear enzyme of topoisomerase I (11). Camptothecin is poorly water soluble with low *in vivo* efficiency as well as severe toxic side effects; therefore in order to improve its pharmaceutical properties, irinotecan as a camptothecin derivative was developed with broad and high antitumor activity *in vivo* and in clinical situation (12,13). All the analogues of camptothecin derivatives share some same characteristics such as a planner five-ring aromatic system with a lactone moiety. According to structure-activity studies, preservation of the lactone ring of camptothecins is essential for their antitumor activity. However, all analogues of camptothecin undergo a pH-dependent, rapid and reversible hydrolysis that changes closed ring lactone to the inactive hydroxyl carboxylated form that loses antitumor properties. In lower pH, the predominant structure is lactone, but at higher pH (like physiological pH), favors the carboxylated form (14,15).

Generraly,oral drug delivery systems are more preferable than the intravenous systems, so there has been increasing efforts to develop oral drug delivery in oncology (16). In order to develop oral anticancer treatments, drug stability as well as drug absorption through the GI lumen must be considered (17). Intravenous administration of irinotecan has indicated significant clinical activity in colorectal cancer treatment. In animals, regular oral administration of camptothecins has shown reduced toxicity as well as much more desirable profiles. Irinotecan can be transformed in to its active form, SN-38, in the liver by carboxyl esterase. Because orally administered drugs will enter the liver through portal vein, irinotecan can be converted to SN-38. Thus, oral administration of irinotecan may be a more desirable route in colorectal cancer therapy (18,19). The aim of the present study was to synthesize β-LG nanovehicles for oral administration of irinotecan. The size, shape, drug loading efficiency, and release kinetics of the nanostructures containing irinotecan were evaluated. Physicochemical characterization of the complex was assessed by dynamic light scattering (DLS), scanning electron microscopy (SEM), and the Fourier-transform infrared (FTIR) study. In addition, binding sites of irinotecan on β-LG were analyzed using molecular docking approach.

MATERIALS AND METHODS

Materials

β-LG and irinotecan hydrochloride were prepared from Sigma-Aldrich Co. (St. Louis, Mo, USA). NaOH, KH_2PO_4, and NaCl were of analytical grade from Merck (Darmstadt, Germany). 3-(4,5- dimethyl- thiazol-2yl)-2,5-diphenyl tetrazolium bromide (MTT), and dimethyl sulfoxide (DMSO) were purchased from Sigma-Aldrich Co. (St. Louis, Mo, USA). The HT29 (human colon cancer cell line) and AGS (gastric adenocarcinoma cell line) were purchased from the National Cell Bank, Pasteur Institute of Iran, Tehran, I.R. Iran.

All other chemicals used in this study were of analytical grade.

Preparation of β-lactoglobulin-irinotecan nanocarriers

In order to synthesize the β-LG nanocarrier, first, protein solution was prepared in a concentration of 0.11 mg in 3 mL phosphate buffer (0.01 M) at different pHs of 3.5, 5, and 7.5. The beakers containing β-LG solutions were kept at room temperature with continuous magnetic stirring (60 rpm). At intervals of 20 min, the drug was added to the β-LG solutions. The different concentrations of irinotecan (5, 30, and 60 μM) were mixed with the β-LG solution and stirred for 3 h. The optimum formulation was selected according to the size of nanoparticle, percent of drug loading, as well as encapsulation efficiency (20).

Physicochemical characterization of β-lactoglobulin-irinotecan complex

Dynamic light scattering analysis

DLS was used to measure the hydrodynamic diameter of the nanocarriers using Zetasizer Nano ZS (Malvern Instruments, Malvern, Worcestershire, UK). The measurements were performed in triplicate at 25 °C.

Scanning electron microscopy

The morphological characteristics of the β-LG-nanoparticles were examined by SEM (Phillips XL30, Netherlands). One drop of nanoparticle sample was thinly sprinkled on a metal slab and vacuum coated with a thin layer of gold under argon atmosphere. Subsequently, the coated sample was scanned and photomicrographs were obtained.

Fourier-transform infrared spectroscopy

FTIR spectra of free drug, free protein, and β-LG-irinotecan nanoparticles were recorded on KBr pellets with a FTIR spectrophotometer (Prestige 21, Shimadzu, Japan).

Entrapment efficiency and drug loading

In order to evaluate the percentage of encapsulation efficiency (EE) and drug loading, the solution of β-LG nanoparticles containing irinotecan was dialyzed against phosphate buffer solution (0.01 M, pH 7.5). The concentration of irinotecan was measured using UV-visible spectrophotometer (UV mini 1240, Shimadzu, Japan) at 254 nm. The amount of untrapped drug was measured and subtracted from the initial drug used. The EE and drug loading values were calculated using equations (1) and (2), respectively.

$$EE\ (\%) = [W_a - W_f / W_a] \times 100 \ldots\ldots\ldots \quad (1)$$

$$\text{Drug loading } (\%) = [(W_a - W_f) / (W_a - W_f + W_p)] \times 100 \quad (2)$$

where, W_a, W_f, and W_p are the weight of drug initially added into the system, weight of untrapped drug, and weight of the protein added into the system, respectively (20,21).

In vitro drug release

Studies on irinotecan release from β-LG nanoparticles were performed in phosphate buffer solution (0.01 mM) with various pH using dialysis tube (cut-off: 12 kDa).

Simulated gastric fluid (SGF), simulated duodenum fluid, simulated terminal ileum fluid (STIF), and the simulated colon fluid were prepared. The pH of 4.5 was used to simulate the duodenum fluid after emptying of gastric content to the small intestine. The pH 7.0 was selected to simulate the pH of the colon fluid, and pH 7.4 was selected to simulate the terminal ileum fluid (22,23). SGF as an artificial dissolution medium was obtained by dissolving 2.0 g of sodium chloride and 3.2 g of purified pepsin in 7.0 mL of hydrochloric acid in 1 L of deionized water (pH ~ 1.2). STIF was prepared by dissolving 6.8 g KH_2PO_4 and 10 g of pancreatine in 250 mL of water. Afterwards, 77 mL of NaOH solution (1 N) was added to the above solution, and volume was brought to 1 L (pH ~ 6.8). Nanoparticles in dialysis membranes were then incubated in 50 mL of media at 37 °C stirred by magnetic bar at 40 rpm. The pH sensitivity and the time dependency of irinotecan release profile from optimum formulation in the gastrointestinal fluid were investigated. Samples of 1 mL, which were replaced with fresh medium, were taken at specified

time intervals and the drug concentration in the samples was determined using a spectrophotometer at 254 nm. The release tests were performed for at least three separate experiments and the mean value of cumulative percentage of the calculated drug was plotted against time.

In vitro drug release kinetics

In order to investigate the mechanism of irinotecan release from nanocarrier, *in vitro* release data were analyzed using various kinetic models. The zero order kinetic model (3) describes the release from the system where the release rate is independent of the dissolved substance concentration.

$$C_t = C_0 + K_0 t \quad (3)$$

where, C_0 is the initial concentration of the drug, C_t is the cumulative percentage of drug released at time "t" and K_0 is zero-order release constant (24).

The first order release (equation 4) defines where the release rate is concentration dependent (25).

$$\text{Log } C_t = \text{Log } C_0 + K_1 t/2.303 \quad (4)$$

where, K_1 is the first-order release constant.

Higuchi described the release of drugs from matrix as a square root of time-dependent process based on the Fickian diffusion (26).

$$C_t = C_0 + K_H t^{1/2} \quad (5)$$

where, K_H is the Higuchi constant.

The Hixson-Crowell cube root law defines the release from systems by dissolution where there is a change in surface area and diameter of the particles:

$$(W_0)^{1/3} - (W_t)^{1/3} = K_{HC} t \quad (6)$$

where, K_{HC} is the Hixson-Crowell constant, W_0 is the initial amount of the drug in the pharmaceutical dosage form and W_t is remaining amount of the drug in the pharmaceutical dosage form (25,27).

Korsmeyer *et al*. derived a simple relationship, the Korsmeyer-Peppas model, which described drug release from a polymeric system:

$$C_t = K_{KP}.t^n \quad (7)$$

where, K_{KP} is the Korsmeyer-Peppas constant and n is the release exponent describing the drug release mechanism. Exponent "n" indicates the mechanism of drug release calculated through the slope of the straight line. Korsmeyer *et al*. characterized "n" value for release mechanisms as, $n < 0.5$ for Fickian diffusion and higher values of n between 0.5 and 1.0, or $n > 1.0$, for mass transfer following a non-Fickian model (28,29).

Modeling was performed using the parameters that offer the match between experimental observations and the nonlinear function. The model that most closely fits the release data was designated based on the correlation coefficient (R^2) in models described above.

Molecular docking and prediction of ligand binding

Molecular docking was carried out using Autodock 4.2 software (30). The three dimensional chemical structure of irinotecan was modeled using the HyperChem 8.0.6 program (31). Geometry optimization of irinotecan was done by selecting "Compute" menu and then "Geometry optimization", which will minimize the energy of the selected molecules. The optimized structure of irinotecan, provided by a semi empirical method of Austin model 1 was used as input for AutoDockTools (30). The crystal structure of *β*-LG (PDB ID: 1BSO) was downloaded from the protein data bank, the structure was modified to remove water molecules and add polar hydrogen atoms and Gasteiger charges. Also, all rotatable bonds for ligand were set up as active and Gasteiger charges were assigned to the irinotecan using AutodockTools. Polar hydrogen atoms were added to the protein and water molecules were removed from the structure. Using AutoGrid tools, the grid maps were generated adequately large to include the internal cavity (calyx) of protein as well as significant regions of the surrounding surface. The docking site on protein target was defined by establishing a grid box with the dimensions of X: 86, Y: 82 and Z: 90 Å. with a grid spacing

of 0.397 Å, centered on X: -3667, Y: 15.556 and Z: 20.222 Å. The grid parameter file and the docking parameter file were set up by the AutoDockTools program. Docking simulations were carried out by AutoDock using a Lamarckian genetic algorithm (30). At the end of the docking simulation, the *β*-LG-irinotecan complex with the lowest binding energy was considered as the most favorable structure of complex.

Cytotoxicity studies

Cytotoxicity of optimized preparation of the β-LG-irinotecan nanoparticles was measured by MTT test to assess the viability of the cells (32). The HT29 and AGS cells were seeded in 96-well plates at a density of 1.5×10^4 cells/well and incubated for 24 h to allow sufficient adhesion. The different concentration of the β-LG-irinotecan nanoparticles, free drug, and protein were added to grown cells, in three replicates and incubated for 24 h. After this incubation, cells were washed with phosphate buffered saline and 20 µL of MTT dye solution (10% in phosphate buffer, pH 7.4) was added to each well. The plates were incubated at 37 °C and 5% CO_2 for an additional 3 h. The medium was discarded and formazan crystals were solubilized by adding 100 µL of DMSO and the solution was vigorously mixed to dissolve tetrazolium dye. The cell viability was measured at 570 nm (reference wavelength 630 nm) in microplate reader (Bio-Tek, ELX 800, Winooski, VT).

RESULTS

Preparation and characterization of β-lactoglobulin-irinotecan nanoparticles

To achieve an optimum formulation, various concentrations of β-LG and irinotecan in different pH conditions were prepared (Table 1). The optimum formulation of β-LG nanocarrier obtained using β-LG (2 µM) and irinotecan (30 µM) in 0.01 mM phosphate buffer under the experimental condition mentioned earlier. To evaluate the effect of pH on the size of nanoparticles, the size of nanoparticles was measured in various pHs, 3.5 (pH < pH_i of β-LG), 5 (pH ~ pH_i of β-LG), and 7.5 (pH > pH_i of β-LG). The isoelectric point (pH_i) of β-LG is 5.2 at which the protein has no net charge (20,33). The results of size measurements are shown in Fig. 1. Quantitative results indicate that at pH 5, the size of the β-LG nanocapsules is larger than those at pHs 3.5 and 7.5. The optimum formulation shows the EE and drug loading parameters in the range of 84.33 ± 5.03% and 30.63 ± 4.16%, respectively (Table 2).

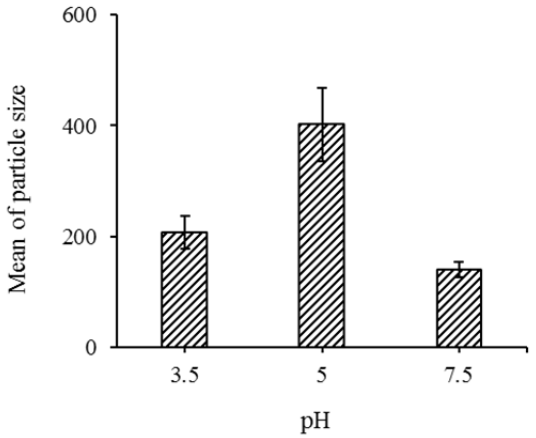

Fig. 1. Mean diameters of β-lactoglobulin nanoparticles prepared in different pH values of phosphate buffer solutions.

Scanning electron microscopy

SEM image of the sample containing prepared nanocarrier is shown in Fig. 2. The image shows spherical shape and smooth surface with particle size in nanometric range. SEM technique confirms that the nanocarrier is globular and well dispersed. The size measurement of the nanoparticle determined by SEM is supported well by DLS experiment.

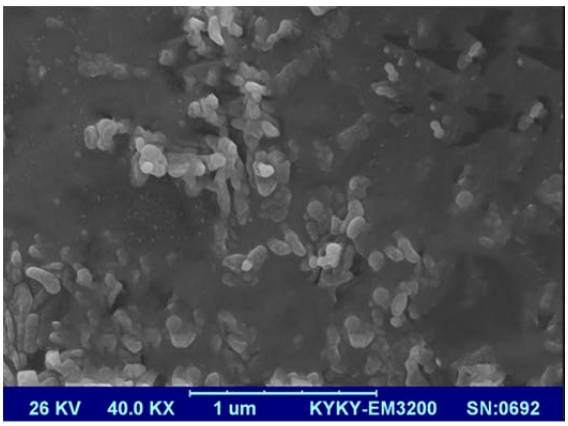

Fig. 2. Scanning electron microscopy image of the irinotecan loaded on β-lactoglobulin nanocarrier

Table 1. Experimental design and size determination.

β-lactoglobulin (µM)	Irinotecan (µM)	pH	Size (nm)	PDI
2	5	3.5	163.56 ± 35.95	0.70 ± 0.15
2	30	3.5	207.10 ± 29.09	0.42 ± 0.09
2	60	3.5	251.43 ± 42.06	0.54 ± 0.13
2	5	5.0	350.34 ± 42.41	0.89 ± 0.08
2	30	5.0	402.33 ± 66.52	0.66 ± 0.11
2	60	5.0	471.60 ± 27.96	0.72 ± 0.13
2	5	7.5	132.26 ± 41.62	0.47 ± 0.07
2	30	7.5	139.86 ± 13.76	0.27 ± 0.10
2	60	7.5	158.83 ± 27.38	0.33 ± 0.06

Data are expressed as mean ± SD of three measurements. PDI, polydispersity index

Table 2. Entrapment efficiency and drug loading of β-lactoglobulin nanoparticles in different drug concentrations. Data are expressed as mean ± SD of three measurements.

β-lactoglobulin (µM)	Irinotecan (µM)	Entrapment efficiency	Drug loading (%)
2	5	52.13 ± 2.52	12.04 ± 1.91
2	30	84.33 ± 5.03	30.63 ± 4.16
2	60	61.09 ± 4.19	28.09 ± 3.97

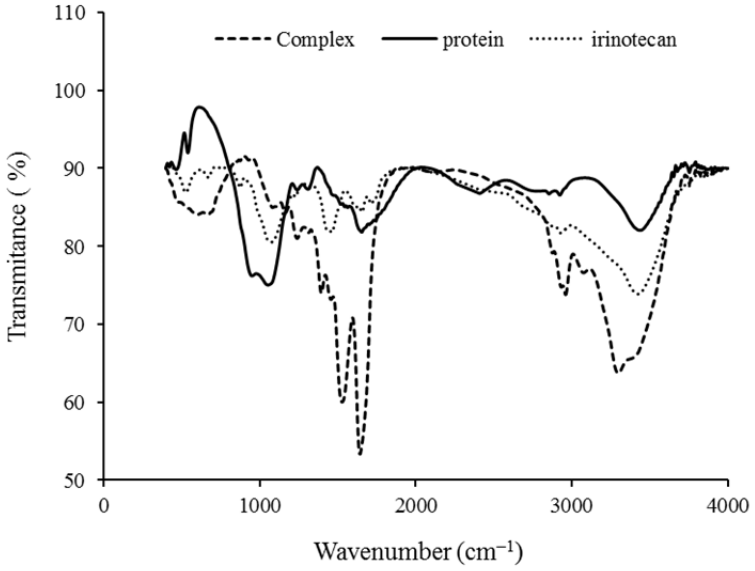

Fig. 3. Fourier-transform infrared spectra of β-lactoglobulin protein, irinotecan, and β-lactoglobulin-irinotecan complex.

Fourier-transform infrared spectra of nanoparticle

IR spectra of proteins show a number of amide bands (I, II, and III) indicating the different modes of the peptide bond vibrations (34). The peaks of amide I (mainly as a result of C=O bond stretching) and amide II (due to C-N bond stretching coupled with N-H bending mode) appear in the regions of 1600-1700, and 1500-1600 cm^{-1}, respectively (35). Figure 3 shows the FTIR spectra of free β-LG, irinotecan, and β-LG-irinotecan complex. The peak position of amide I and II and C-N stretching moved from 1623 to 1643, 1545 to 1527, and 2854 to 2873 cm^{-1}, respectively, in β-LG-irinotecan complex in comparison with free β-LG. As depicted in Fig. 3, the FTIR spectrum of

the protein revealed a broad band at approximately 2407 cm^{-1}, however, it is not present in the spectrum of β-LG-irinotecan complex. The FTIR spectrum of irinotecan bands at 1076 and 1431 cm^{-1}, disappeared after binding to β-LG.

In vitro drug release

In order to investigate the drug release behavior of drug in β-LG nanvehicles, samples were incubated in different release medias (pHs: 1.2, 4.5, 7.0, and 7.5) and were assessed by UV spectrophotometry. It can be assumed that β-LG nonvehicle has a pH-responsive release behavior for included drug. Figure 4 demonstrates irinotecan release profiles up to 24 h of incubation period. The percent of drug release at pH 7.4 is more than pHs 1.2, 4.5, and 7.0. Figure 5 shows the release pattern of irinotecan from nanocarrier in SGF (pH 1.2) and STIF (pH 7.4). Approximately, 20% of the drug was released in the SGF and 80% in STIF over a period of 24 h. It can be concluded that in the conditions similar to *in vivo*, the release behavior of the drug from developed nanocarrier in the STIF condition is significantly higher than SGF. The result is in good agreement with release profile in phosphate buffer at different pHs.

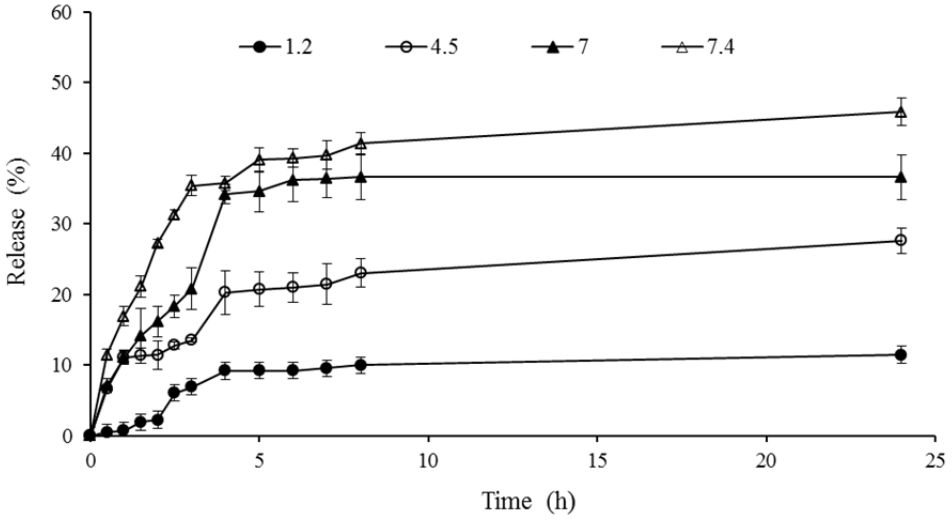

Fig. 4. *In vitro* release profiles of irinotecan from β-lactoglobulin nanoparticles in 10 mM phosphate buffer solutions at pH 1.2, 4.5, 7.0, and 7.4 (simulated gastrointestinal system) at 37 °C.

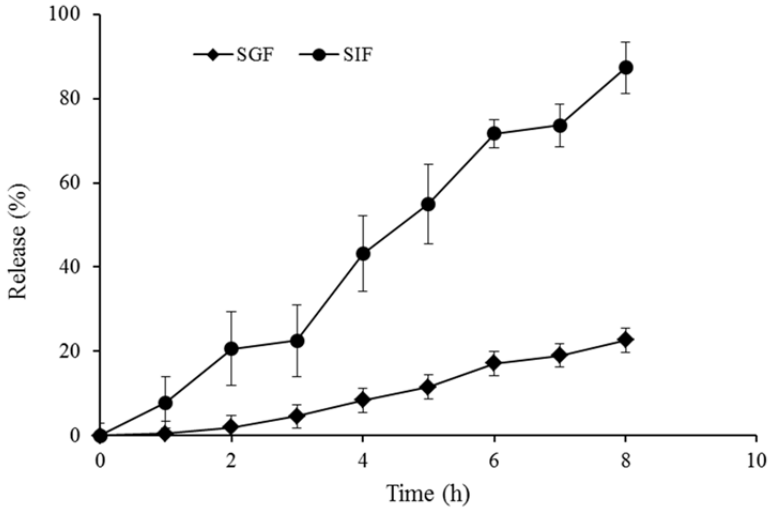

Fig. 5. Release profile of drug from nanocarrier in simulated gastric fluid and simulated intestinal fluid conditions at 37 °C after 8 h.

Table 3. R-squared (R^2) values of release kinetics according to various equations.

pH	Zero-order	First-order	Higuchi	Hixon-Crowell	Korsmeyer-Peppas
1.5	0.477	0.512	0.884	0.484	0.814
4.5	0.639	0.623	0.921	0.650	0.931
7.0	0.392	0.425	0.938	0.398	0.850
7.5	0.450	0.480	0.880	0.494	0.846

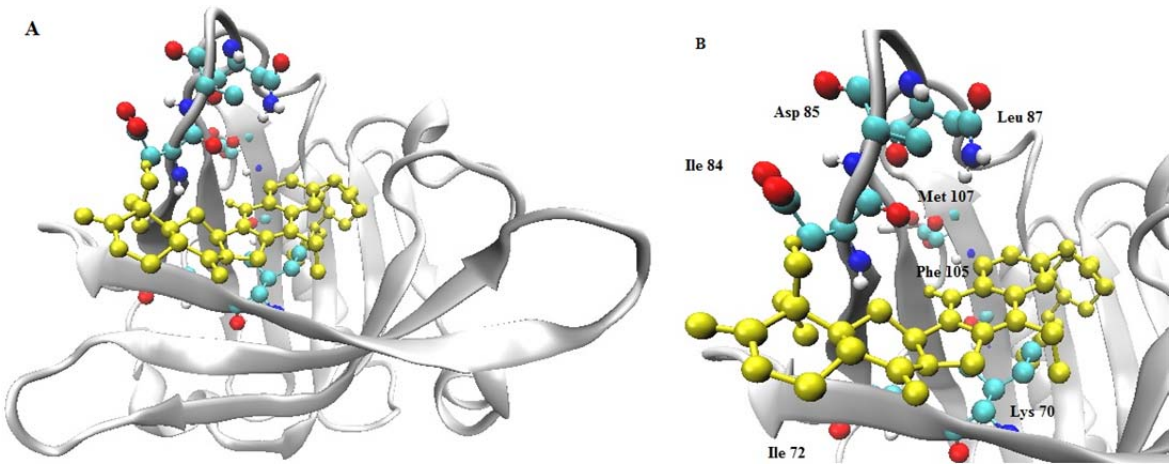

Fig. 6. (A) Structural rendering of the docked β-lactoglobulin (silver backbone) and β-lactoglobulin-irinotecan (yellow structure). (B) Significant interacting residues are numbered as per the original PDB file. Residues are shown in ball-and-sticks scheme. Final conformation obtained after energy minimization has been prepared using the program VMD. (For interpretation of the references to colour in this figure legend, the reader is referred to the web version of this article).

In this study, the release kinetics and mechanisms of irinotecan release from β-LG nanovehicles were evaluated using several mathematical models (zero order, first order, Higuchi, Hixson-Crowell, and Korsmeyer-Peppas). Table 3 demonstrates correlation values (R^2) and release parameters obtained from the model fitting results of the release profiles. According to correlation values, release data well fits to the Higuchi model at all pH values indicating release of irinotecan by a diffusion mechanism. For the optimized formulation, the R^2 value of Higuchi equation is the most probable model comparing to the other models that indicate the drug release is determined by the square root of the time.

Docking studies

In order to get more information about binding sites of irinotecan on β-LG, molecular docking was employed to simulate the drug and protein interaction. At the end of the docking simulation, the β-LG-irinotecan complex with the lowest docked energy (**(**ΔG_{bind}, -7.04 kJ/mol) was adopted as the most favorable structure of the protein complex. Figure 6 shows a stereo schematic of the β-LG structure with the positions of irinotecan. Based on the results presented in Fig. 6A, there is an internal cavity (calyx) which can readily accommodate irinotecan with the best docked energy. The drug molecule is located within the internal cavity of β-LG adjacent to Ile-84, Leu-87, Asp-85, Met-107, Phe-105, Lys-70, and Ile-72 residues (Fig. 6B). The most residues which are located in the cavity of the β-LG are hydrophobic, such as Val-41, Leu-87, Met-107, Ile-84, Phe-82, Leu-54, Phe-105, Ile-56, Val-92, Ile-72, and Leu-58 (36).

Schematic representations of hydrophobic contacts of β-LG with irinotecan are depicted in Fig. 7. Residues that are close to irinotecan also demonstrated that hydrophobic forces predominate during irinotecan interaction with β-LG.

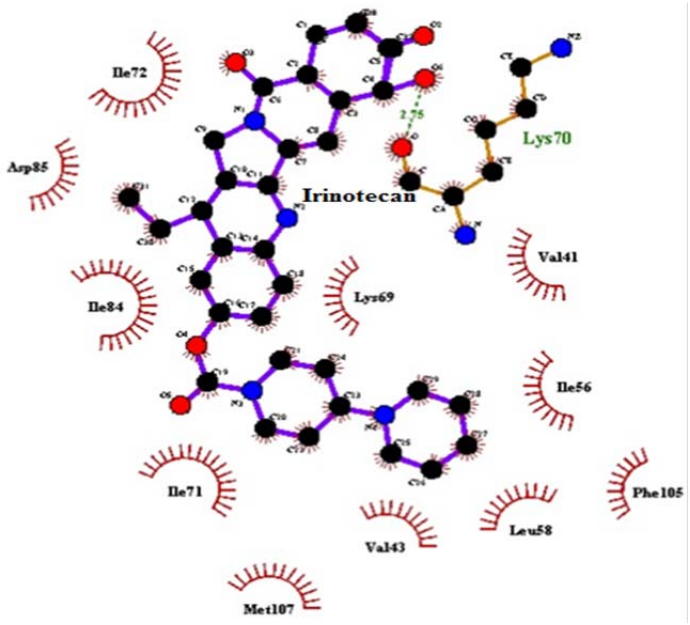

Fig. 7. Two dimensional schematic representations of β-lactoglobulin-irinotecan-irinotecan complex. Drawings were generated using LIGPLOT v.1.4 (40,41).

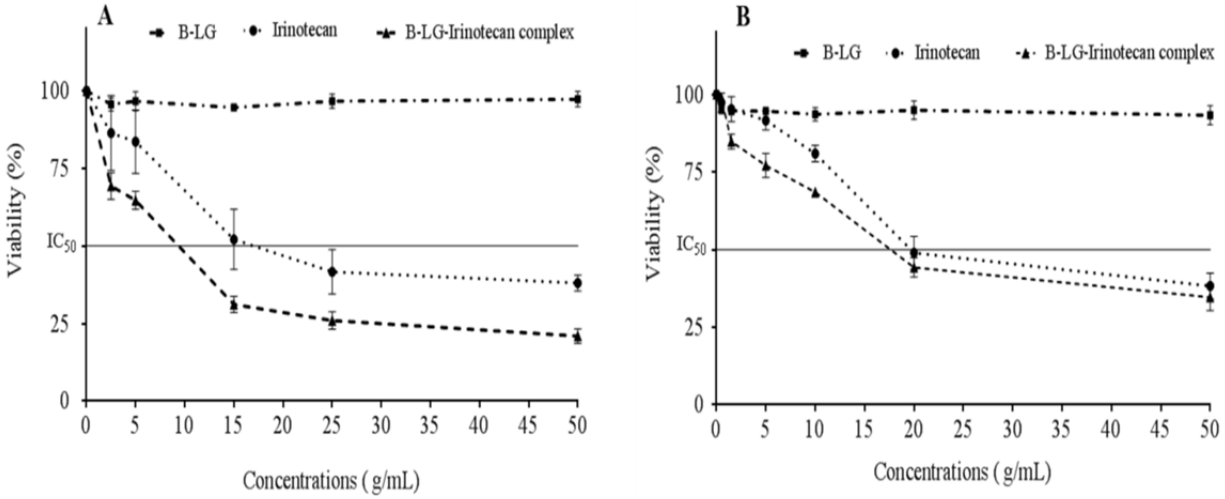

Fig. 8. The effect of β-lactoglobulin (β-LG), Irinotecan, and β-LG-irinotecan nanoparticle concentrations on viability of (A) AGS and (B) HT-29 cells which was examined by MTT assay.

Cell viability assay

Cell viability was assessed using the MTT assay. The MTT assay is based on cleavage of soluble yellow tetrazolium rings and formation of insoluble purple formazan crystals by mitochondrial enzyme in viable cells. Therefore, the amount of formazan formed is directly proportional to the number of viable cells (37). The *in vitro* anti-tumor activity of the irinotecan-β-LG nanoparticle was studied on HT-29 and AGS cell lines after 24 h of exposure to different concentrations of irinotecan and nanoparticles. As shown in Fig. 8, β-LG had no cytotoxic effect on HT-29 and AGS cells.

DISCUSSION

It is obvious that, there is a significant relationship between pH values and size of the synthesized β-LG-irinotecan nanoparticle. At pH 5 which is very close to the pI of

β-LG (20), the number of positively-charged side chains is equal to the number of negatively-charged side chains that indicates a balance between various attractive forces (*e.g.*, van der Waals, hydrophobic, and electrostatic interactions between oppositely charged groups) and various repulsive forces (*e.g.*, electrostatic interactions between similarly charged groups) (38). At pH values lower than the pI (pH 3.5), more basic side chains of amino acids become protonated leading to the protein with net positive charge. Similarly, at pH values higher than the pI (pH 7.5), more acidic side chains become deprotonated with a net negative charge and high repulsive forces between similar charged groups will inhibit interactions between proteins. It can be assumed that β-LG nanovehicle behaves as a pH-responsive release behavior for included drug. The release profiles at pH 7.0 to 7.4 within 24 h clearly indicate that the drug release from nanovehicles was strongly influenced by the pH. As shown in the release results, the burst release is decreased with a decline in pH that demonstrates preservation of the drug in the nanovehicles at low pH. The initial burst release of irinotecan might be due to a rapid release of weakly adsorbed irinotecan onto the nanoparticle's surface. The more release of drug from β-LG at pH 7.4, which is similar to the intestine pH suggests that this biopolymer may act as suitable nanotransporter which releases anticancer drug in the colorectal section and is able to bypasses stomach acidic environment. Based on the results of FTIR, the peak positions of the amides I and II bands in β-LG IR spectrum shifted slightly due to interaction with irinotecan. In general, FTIR spectroscopy reveals that a partial folding of β-LG structure took place upon interaction with the drug. The molecular docking results demonstrated that the hydrophobic forces are predominating during irinotecan binding to β-LG. We concluded that irinotecan binds to the hydrophobic calyx of β-LG which coincides well with previous investigation (39).

The new synthesized β-LG-irinotecan nanoparticle has higher cytotoxic effects compared to irinotecan in both cancer cell lines. It can be predicted that the active lactone form of drug was maintained inside the nano-carriers, therefore, we observed more inhibitory effect of nanoparticles against the free drug. Based on these findings, nanoparticles were able to transport more drugs into the cells achieving a lower cell viability and greater cytotoxicity compared to free drug after 24 h.

The average IC_{50} values of irinotecan in the formulation for two cell lines showed that irinotecan as the complex pose much more cytotoxicity in AGS cells rather than free drug (i.e. IC_{50} value of 7.83 ± 1.34 µg/mL in irinotecan-β-LG complex compared to IC_{50} values of 17.84 ± 1.03 µg/mL for free drug form, respectively, $P< 0.01$). In HT29 cell line; there is no significant difference between two forms of drug (i.e. IC_{50} value of 19.45 ± 4.60 µg/mL and 21.64 ± 5.83 µg/mL for in irinotecan-β-LG complex and free drug form, respectively.

CONCLUSION

In this paper, it was verified that irinotecan loaded on β-LG nanocarrier can be utilized in colorectal cancer treatment using the physical inclusion method. The results obtained from the DLS measurements have shown that at pH 7.5, nanoparticles have the smallest size. The *in vitro* release studies shows that the β-LG nanocarrier containing the drug are significantly pH sensitive and at pH 7.5, which is the pH level for the stimulated terminal fluid, the nanocarrier showed maximum release. Our result suggests that this new synthesized nanoparticle can induce cytotoxic effects on cancerous cell lines, thus it has effectively inhibiting tumor progression potential compared to free form of anticancer drug.

ACKNOWLEDGMENTS

This work was financially supported (Grant No. 94048) by Vice Chancellor of Research and Technology Center, Kermanshah University of Medical Sciences, Kermanshah, I.R. Iran.

REFERENCES

1. Mazzaferro S, Bouchemal K, Ponchel G. Oral delivery of anticancer drugs III: formulation using drug delivery systems. Drug Discov Today. 2013;18(1-2):99-104.
2. Caillard R, Boutin Y, Subirade M. Characterization of succinylated β-lactoglobulin and its application as the excipient in novel delayed release tablets. Int Dairy J. 2011;21(1):27-33.
3. Kepple rJK, Sonnichsen FD, Lorenzen PC, Schwarz K. Differences in heat stability and ligand binding among β-lactoglobulin genetic variants A, B and C using (1)H NMR and fluorescence quenching. Biochim Biophys Acta. 2014;1844(6):1083-1093.
4. Halder UC, Chakraborty J, Das N, Bose S. Tryptophan dynamics in the exploration of micro-conformational changes of refolded β-lactoglobulin after thermal exposure: a steady state and time-resolved fluorescence approach. J Photochem Photobiol B. 2012;109:50-57.
5. Caillard R, Remondetto GE, Mateescu MA, Subirade M. Characterization of amino cross-linked soy protein hydrogels. J Food Sci. 2008;73(5): C283-C291.
6. Caillard R, Petit A, Subirade M. Design and evaluation of succinylated soy protein tablets as delayed drug delivery tablets. Int J Biol Macromol. 2009;45(4):414-420.
7. KonumaT, Sakurai K, GotoY. Promiscuous binding of ligands by beta-lactoglobulin involves hydrophobic interactions and plasticity. J Mol Biol. 2007;368(1):209-218.
8. ChakrabortyJ, DasN, HalderUC. Unfolding diminishes fluorescence resonance energy transfer (FRET) of lysine modified β-lactoglobulin: Relevance towards anti-HIV binding. J Photochem Photobiol B. 2011;102(1):1-10.
9. Le Maux S, Bouhallab S, Giblin L, Brodkorb A, Croguennec T. Bovine β-lactoglobulin/fatty acid complexes: binding, structural, and biological properties. Dairy Sci Technol. 2014;94(5):409-426.
10. QinB Y, Bewley MC, Creamer LK, Baker HM, Baker EN, Jameson GB. Structural basis of the Tanford transition of bovine beta-lactoglobulin. Biochemistry. 1998;37(40):14014-14023.
11. Rivory LP. New drugs for colorectal cancer-mechanisms of action. Exp Clin Pharmacol. 2005;25(5):108-110.
12. Potmesil M. Camptothecins: from bench research to hospital wards. Cancer Res. 1994;54(6): 1431-1439.
13. Kaneda N, Nagata H, Furuta T, Yokokura T. Metabolism and pharmacokinetics of the camptothecin analogue CPT-11 in the mouse. Cancer Res. 1990;50:1715-1720.
14. Derakhshandeh K, Erfan M, Dadashzade S. Encapsulation of 9-nitrocamptothecin, a novel anticancer drug, in biodegradable nanoparticles: factorial design, characterization and release kinetics. Eur J Pharm Biopharm. 2007;66(1):34-41.
15. Fassberg J, Stella VJ. A kinetic and mechanistic study of the hydrolysis of camptothecin and some analogues. J Pharm Sci. 1992;81(7):676-684.
16. Diasio RB. Current status of oral chemotherapy for colorectal cancer. Oncology (Williston Park). 2001;15(3 Suppl 5):16-20.
17. Sharma S, Saltz LB. Oral chemotherapeutic agents for colorectal cancer. Oncologist. 2000;5(2):99-107.
18. Houghton PJ, Stewart CF, Zamboni WC, Thompson J, Luo X, Danks MK, *et al*. Schedule-dependent efficacy of camptothecins in models of human cancer. Ann N Y Acad Sci. 1996;803:188-201.
19. Drengler RL, Kuhn JG, Schaaf LJ, Rodriguez GI, Villalona-Calero MA, Hammond LA, *et al*. Phase I and pharmacokinetic trial of oral irinotecan administered daily for 5 days every 3 weeks in patients with solid tumors. J Clin Oncol. 1999;17(2):685-696.
20. Ghalandari B, Divsalar A, Saboury AA, Parivar K. The new insight into oral drug delivery system based on metal drugs in colon cancer therapy through β-lactoglobulin/oxali-palladium nanocapsules. J Photochem Photobiol B. 2014;140:255-265.
21. Kashanian S, Hemati Azandariyani A, Derakhshandeh K. New surface-modified solid lipid nanoparticles using N-glutaryl phosphatidyl ethanolamine as the outer shell. Int J Nanomedicine. 2011;6:2393-2401.
22. McConnell EL, Fadda HM, Basit AW. Gut instincts: explorations in intestinal physiology and drug delivery. Int J Pharm. 2008;364(2):213-226.
23. EvansDF, Pye G, Bramley R, Clark AG, Dyson TJ, Hardcastle JD. Measurement of gastrointestinal pH profiles in normal ambulant human subjects. Gut. 1998;29(8):1035-1041.
24. Varelas CG, Dixon DG, Steiner CA. Zero-order release from biphasic polymer hydrogels. J Control Release. 1995;34(3):185-192.
25. Costa P, Lobo JMS. Modeling and comparison of dissolution profiles. Eur J Pharm Sci. 2001;13(2):123-133.
26. Higuchi T. Mechanism of sustained-action medication, theoretical analysis of rate of release of solid drugs dispersed in solid matrices. J Pharm Sci. 1963;52:1145-1149.
27. Hixson AW, Crowell JH. Dependence of reaction velocity upon surface and agitation. Ind Eng Chem Res. 1931;23(8):923-931.
28. Prodduturi S, Urman KL, Otaigbe JU, Repka MA. Stabilization of hot-melt extrusion formulations containing solid solutions using polymer blends. AAPS PharmSciTech. 2007;8(2):E152-E161.
29. Barzegar-Jalali M, Adibkia K, Valizadeh H, Shadbad MR, Nokhodchi A, Omidi Y, *et al*. Kinetic analysis of drug release from nanoparticles. J Pharm Pharm Sci. 2008;11(1):167-177.
30. Morris GM, Goodsell DS, Halliday RS, Huey R, Hart WE, Belew RK, *et al*. Automated docking using Lamarckian genetic algorithm and an empirical binding free energy function. J Comput Chem. 1998;19:1639-1662.

31. Froimowitz M. HyperChem: a software package for computational chemistry and molecular modeling. Biotechniques 1993;14(6):1010-1013.
32. Liu Y, Peterson DA, Kimura H, Schubert D. Mechanism of cellular 3-(4,5-dimethylthiazol-2-yl)-2,5-diphenyltetrazolium bromide (MTT) reduction. J Neurochem. 1997;69(2):581-593.
33. Adams JJ, Anderson BF, Norris GE, Creamer LK, Jameson GB. Structure of bovine beta-lactoglobulin (variant A) at very low ionic strength. J Srtuct Biol. 2006;154(3):246-254.
34. Naik PN, Nandibewoor ST, Chimatadar SA. Non-covalent binding analysis of sulfamethoxazole to human serum albumin: Fluorescence spectroscopy, UV-vis, FT-IR, voltammetric and molecular modeling. J Pharm Anal. 2015; 5(3): 143-152.
35. Gao W, Li N, Chen Y, Xu Y, Lin Y, Yin Y, *et al*. Study of interaction between syringin and human serum albumin by multi-spectroscopic method and atomic force microscopy. J Mol Struct. 2010;983(1-3):133-140.
36. Sawyer L, Brownlow S, Polikarpov I, Wu SY. β-Lactoglobulin: structural studies, biological clues. Int Dairy J. 1998;8(2):65-72.
37. Shukla S, Jadaun A, Arora V, Sinha RK, Biyani N, Jain V. *In vitro* toxicity assessment of chitosan oligosaccharide coated iron oxide nanoparticles. Toxicol Rep.2014;2:27-39.
38. Chanasattru W, Jones OG, Decker EA, McClements DJ. Impact of cosolvents on formation and properties of biopolymer nanoparticles formed by heat treatment of β-lactoglobulin-Pectin complexes. Food Hydrocoll. 2009;23(8):2450-2457.
39. Bijari N, Ghobadi S, Derakhshandeh K. Irinotecan binds to the internal cavity of beta-lactoglobulin: A multi-spectroscopic and computational investigation. J Pharm Biomed Anal. 2017;139:109-115
40. Bijari N, Moradi S, Ghobadi S, Shahlaei M. Elucidating the interaction of letrozole with human serum albumin by combination of spectroscopic and molecular modeling techniques. Res Pharm Sci. 2018;13(4):304-315.
41. Wallace AC, Laskowski RA, Thornton JM. LIGPLOT: a program to generate schematic diagrams of protein-ligand interactions. Protein Eng. 1995;8(2):127-134.